Available online at www.sciencedirect.com

SCIENCE DIRECT®

Biochimica et Biophysica Acta 1666 (2004) 190–204

BIOCHIMICA ET BIOPHYSICA ACTA
BBA

http://www.elsevier.com/locate/bba

Review

The alignment, structure and dynamics of membrane-associated polypeptides by solid-state NMR spectroscopy

Burkhard Bechinger*, Christopher Aisenbrey, Philippe Bertani

Faculté de chimie, Institut le Bel, 4, rue Blaise Pascal, 67000 Strasbourg, France

Received 30 March 2004; accepted 6 August 2004
Available online 11 September 2004

Abstract

Solid-state NMR spectroscopy is being developed at a fast pace for the structural investigation of immobilized and non-crystalline biomolecules. These include proteins and peptides associated with phospholipid bilayers. In contrast to solution NMR spectroscopy, where complete or almost complete averaging leads to isotropic values, the anisotropic character of nuclear interactions is apparent in solid-state NMR spectra. In static samples the orientation dependence of chemical shift, dipolar or quadrupolar interactions, therefore, provides angular constraints when the polypeptides have been reconstituted into oriented membranes. Furthermore, solid-state NMR spectroscopy of aligned samples offers distinct advantages in allowing access to dynamic processes such as topological equilibria or rotational diffusion in membrane environments. Alternatively, magic angle sample spinning (MAS) results in highly resolved NMR spectra, provided that the sample is sufficiently homogenous. MAS spinning solid-state NMR spectra allow to measure distances and dihedral angles with high accuracy. The technique has recently been developed to selectively establish through-space and through-bond correlations between nuclei, similar to the approaches well-established in solution-NMR spectroscopy.
© 2004 Elsevier B.V. All rights reserved.

Keywords: Helix tilt; Chemical shift; Oriented bilayer; Membrane protein; Transmembrane alignment; MAOSS; MAS; Conformation; In-plane helix; Hydrophobic residue; Amphipathic helix; Channel; Antibiotic; vpU; Magainin; Melittin; Alamethicin; Model peptide; Gramicidin; Heteronuclear correlation

Contents

* Corresponding author. Tel.: +33 3 9024 5150; fax: +33 3 9024 5151.
E-mail address: bechinger@chimie.u-strasbg.fr (B. Bechinger).

0005-2736/$ - see front matter © 2004 Elsevier B.V. All rights reserved.
doi:10.1016/j.bbamem.2004.08.008

1. Introduction

Structural information on membrane-associated peptides and proteins remains sparse due to the difficulties encountered during biochemical preparation and the limitations imposed by the classical diffraction and solution NMR methods. Therefore, other biophysical techniques, which allow the investigation of these proteins in their natural environment, remain of utmost importance during the study of this very important class of proteins [1,2]. Among those, solid-state NMR spectroscopy has proven to be a valuable method for the investigation of the structure as well as the dynamics of membrane-associated proteins and peptides (reviewed, e.g. in Refs. [3–12]). Important information such as distances or dihedral angles within membrane proteins, or between integral membrane proteins and their ligands has been obtained [4,5]. Furthermore, the tilt angles of helices with respect to the bilayer normal are accessible using this methodology [13]. The structural investigation of biological macromolecules by solid-state NMR spectroscopy does not require the formation of monocrystals or the fast isotropic re-orientation of molecules, these being prerequisites for diffraction techniques or solution NMR spectroscopy, respectively. The possibility to investigate membrane polypeptides in their natural bilayer environment when at the same time very accurate structural information can be obtained, therefore, is a distinct advantage of solid-state NMR spectroscopy over many other techniques. Solid-state NMR spectroscopy is also sensitive to the molecular dynamics of membrane-associated molecules and therefore provides access to the rate and directionality of molecular exchange.

In the past, solid-state NMR spectroscopy has developed its full strength when it was possible to introduce isotopic labels selectively at specific sites. In such cases, very accurate answers have been obtained for specific questions. However, by measuring a large number of conformational constraints, this approach has also been shown to be suitable for the complete structure determination of membrane-bound peptides [3]. In this work, advantage has been taken of the orientation-dependence of NMR interactions that allow one to extract angular constraints. The anisotropy of NMR interactions remains apparent in immobilized as well as slowly spinning samples but can be abolished by fast spinning around the 'magic angle'. This latter approach has recently resulted in high-resolution correlation spectra and the first solid-state NMR structure of a protein in a microcrystalline environment [14].

2. Some fundamentals of biological solid-state NMR spectroscopy

Although the investigation of small globular proteins in solution by multidimensional solution NMR spectroscopy has become almost routine [15] these techniques fail when proteins or biomolecular complexes exceeding a certain size are investigated [16]. The NMR spectrum of even a small polypeptide, when associated with large macromolecular aggregates such as a phospholipid vesicle or fibrillar structures, exhibit broad unresolved lines when it is merely placed into a test tube and inserted into the NMR coil (Fig. 1A). This is due to the inherent anisotropy of nuclear interactions, which are dependent on the orientation and conformation of the molecule with respect to the magnetic field direction [17–20]. Whereas in solution fast molecular tumbling ensures isotropic averaging of the nuclear interactions, the re-orientational correlation times of molecules associated with extended phospholipid bilayers are directional and slow when compared to the time scales of the chemical shift, dipolar or quadrupolar interactions. As a consequence, the anisotropic properties of these interactions are reflected in the NMR line shapes of bilayer-associated biomolecules or of polypeptide fibrils such as those found in the Alzheimer disease [21–25]. In such spectra the signals that arise from different sites tend to overlap and remain largely unresolved (Fig. 1A).

To overcome this problem two fundamentally different NMR approaches have been established. On the one hand fast spinning of the samples around the 'magic angle' allows one to produce spectra of heteronuclei, which resemble those obtained in solution [26] (Fig. 1C). On the other hand, techniques have been developed in which samples uniaxially oriented relative to the magnetic field direction are obtained [27]. The spectra of these preparations thus reveal orientational differences between the labeled sites [28].

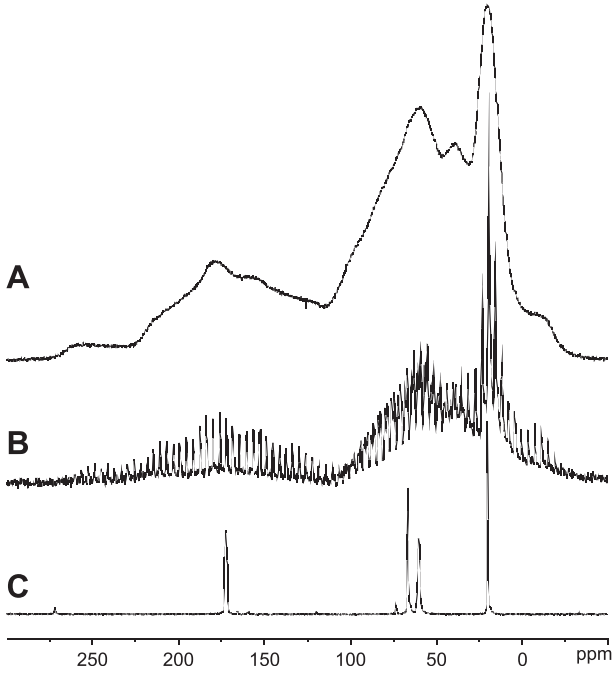

Fig. 1. Proton-decoupled ^{13}C solid-state NMR spectra of (U–^{13}C, U–^{15}N) L-threonine. (A) Static conditions. (B) Same sample when spun around the magic angle at $\omega_r/2\pi$=390 Hz. (C) Same sample when spun around the magic angle at $\omega_r/2\pi$=10 kHz.

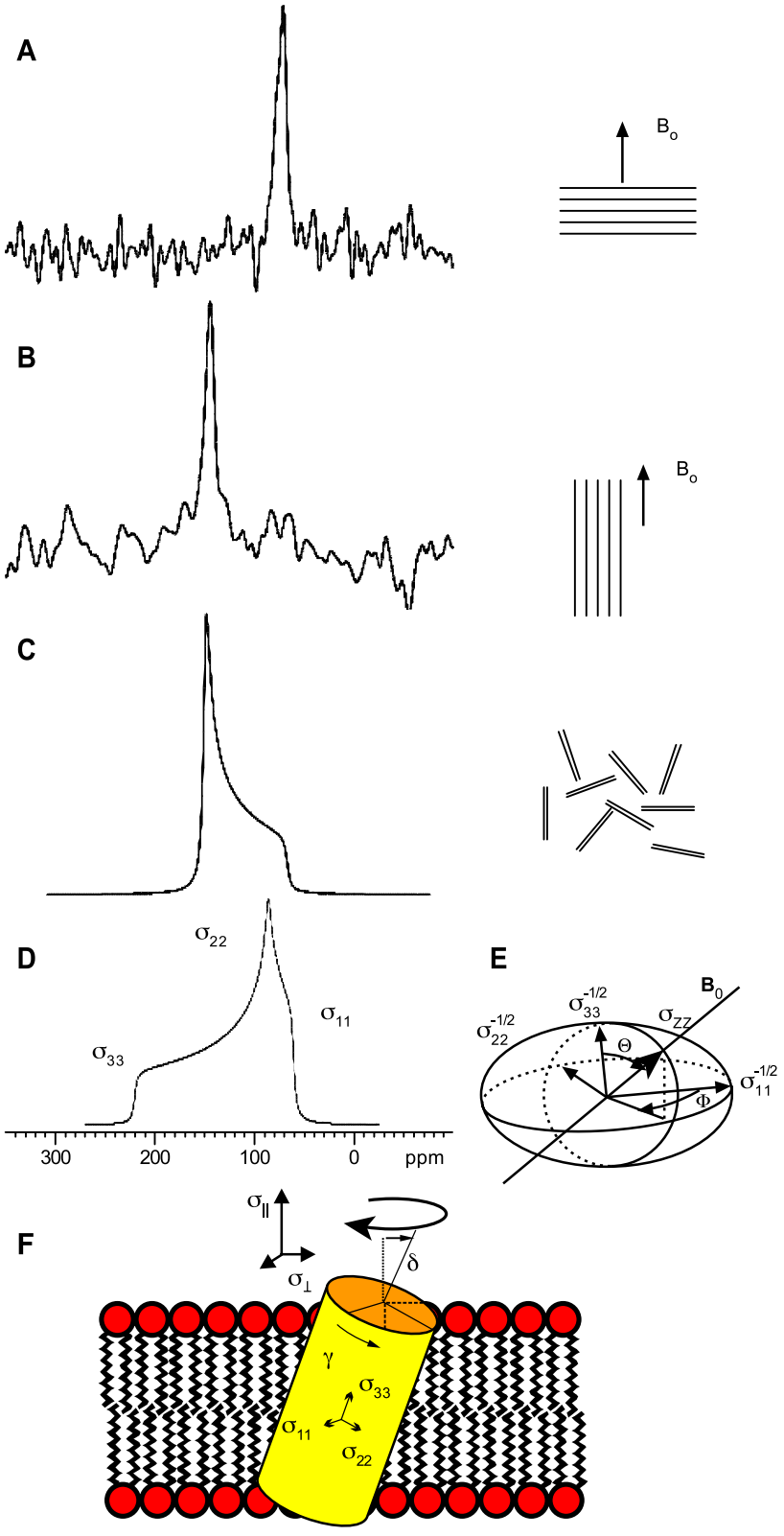

Fig. 2. Proton-decoupled ^{15}N solid-state NMR spectra of the in-plane oriented model peptide LK15 in C20-PC with alignments of the membrane normal parallel (A) and perpendicular (B) to the magnetic field direction. (C) Simulated powder spectra under conditions of fast rotational diffusion around the membrane normal. (D) Static simulated powder spectrum. (E) The ^{15}N chemical shift tensor is represented as an ellipsoid. (F) Transmembrane-inserted helical peptide is represented as a cylinder and the tilt and rotational pitch angles δ and γ are indicated. The approximate alignment of the static tensor elements is shown within the helix. Fast rotation around the bilayer normal results in averaged tensor elements $\sigma_{\parallel}$ and $\sigma_{\perp}$ (cf. text for details).

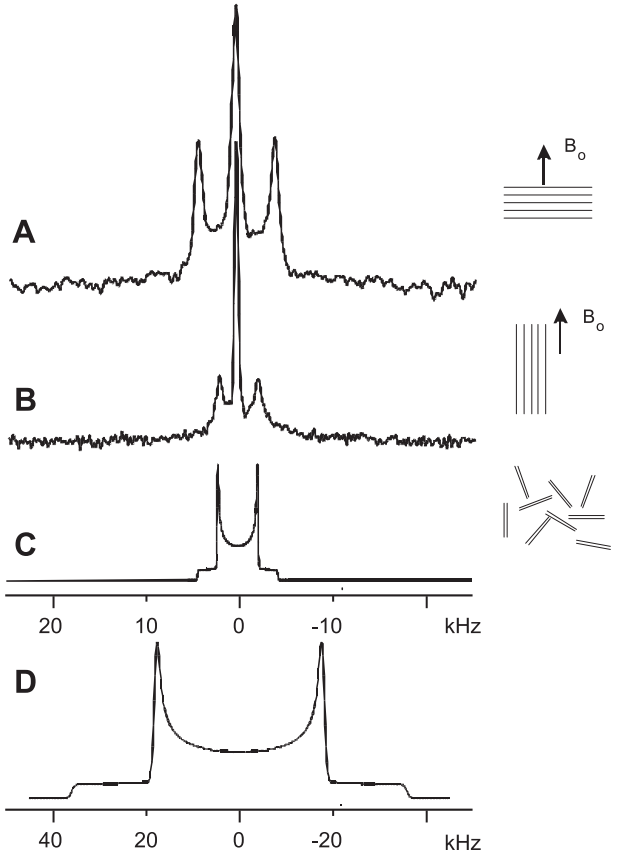

Fig. 3. Deuterium solid-state NMR spectra of the model peptide LK15, labeled with ^{2}H3-alanine at its position and reconstituted in uniaxially oriented C20-PC. The orientation of the membrane normal is parallel (A) and perpendicular to the magnetic field direction (B). The spectrum shown in panel (C) represents the simulation of a non-oriented sample where the helix continues to exhibit fast rotational diffusion around the membrane normal. (D) Simulation of a powder pattern sample at reduced temperature where only averaging around the alanine C_α–C_β bond continues to persist. Note that the spectrum D is shown at a different scale.

Furthermore, selective isotopic labeling (e.g. Refs. [29–33]), multidimensional NMR spectroscopy [34–37], or techniques that decouple or select interactions between nuclear spins [17] help to improve spectral resolution, assignment and structural information [38,39]. Figs. 2 and 3 show ^{15}N and ^{2}H solid-state NMR spectra, respectively, of peptides labeled with ^{15}N or ^{2}H at a single or at equivalent sites and reconstituted into oriented phospholipid bilayers. Furthermore, when the spectra shown in Fig. 2 have been obtained, the interactions of the ^{15}N nucleus with the surrounding protons were decoupled using high-power irradiation at the ^{1}H frequency.

3. Solid-state NMR applied to static samples

To start a more detailed discussion of some of the strategies employed during the investigation of membrane polypeptides using solid-state NMR spectroscopy, let us consider an individual backbone amide labeled with ^{15}N. In this case, the isotopic label is dilute as the distances between ^{15}N nuclei are sufficiently large to ignore all interactions between them. Furthermore, the interactions of the abundant ^{1}H with ^{15}N nuclei are decoupled by high-power irradiation at the ^{1}H frequency. When a dry powder of such a peptide is placed in the NMR coil of a solid-state NMR probe a broad powder-pattern line shape of approximately 160 ppm width is observed (Fig. 2D). This ^{15}N chemical shift anisotropy of a single ^{15}N labeled peptide bond thus is much larger than the width of an individual line of proteins in solution. In the latter case all resonances of the protein backbone resonate within a range of only 20 ppm.

The anisotropic chemical shift interaction is mathematically described by a second rank tensor corresponding to a 3×3 matrix. It is possible to find an orthogonal coordinate system, called the principal axis system (PAS), where only the diagonal elements σ_{11}, σ_{22} and σ_{33} persist. These are the static main tensor elements and correspond to the discontinuities observed in the line shape of powdered samples, where all possible molecular alignments are present at random (Fig. 2D). The tensor reflects the arrangement of the nuclei and bonds within a given molecule and thereby relates the NMR interactions to the molecular coordinates.

This tensor can be transformed into any other coordinate system by applying rotations with the three Euler angles (Φ,Θ,Ψ). An expression of the chemical shift in the new coordinate system is obtained by using the rotation matrices $\mathbf{R}_{ij}$ [18,40,41]:

$$\sigma' = \mathbf{R}\sigma\mathbf{R}^{-1} \tag{1}$$

with

$$\mathbf{R} = \mathbf{R}_{z''}(\Psi)\mathbf{R}_{y'}(\Theta)\mathbf{R}_{z}(\Phi). \tag{2}$$

It is thus possible to relate the orientation of the tensor (molecular frame) relative to the magnetic field direction of the NMR spectrometer (laboratory frame). The component of the chemical shift tensor in direction of the magnetic field direction (zz component) corresponds to the measured NMR chemical shift value. When expressed in terms of Euler angles Θ and Φ (Fig. 2E) and the principal elements of the chemical shift tensor σ_{11}, σ_{22} and σ_{33}, the measurable σ_{zz} amounts to:

$$\sigma_{zz} = \sigma_{11}\sin^2\Theta\cos^2\Phi + \sigma_{22}\sin^2\Theta\sin^2\Phi + \sigma_{33}\cos^2\Theta. \tag{3}$$

Alternatively, the chemical shift value is obtained from direction cosines according to

$$\sigma_{zz} = \sum_{i=1,2,3} \cos^2\vartheta_i\sigma_{ii}. \tag{4}$$

Graphically the chemical shift interaction is represented by an ellipsoid (Fig. 2E), where the lengths of the three main axes represent $1/\sqrt{\sigma_{ii}}$, with σ_{ii} being one of the main tensor elements σ_{11}, σ_{22} and σ_{33} (Fig. 2E). The intersect of the magnetic field vector with the ellipsoid corresponds to

$1/\sqrt{\sigma_{zz}}$ with σ_{zz} being the chemical shift that is apparent at a given orientation of the molecule [13].

The size of the tensor elements as well as their positioning within the molecule are important parameters required to translate solid-state NMR measurements to structural information. Studies on single crystals, establishment of correlations between the chemical shift and the dipolar interactions of directly bonded nuclei, or comparison with known tensors of model compounds allow one to obtain this important piece of information [42–45]. Furthermore, the proton-decoupled ^{15}N chemical shift tensors of alanine or glycine amides have been studied in considerable detail for a number of polypeptides [43,44,46–51]. These static tensors show some modest variation with respect to the secondary structure of the polypeptide chain and the nature of the amino acid side chain [50,52]. Therefore, in this discussion, we will use representative averages of the ^{15}N chemical shift tensor of the peptide bond. When accurate structural information from solid-state NMR is wanted it has proven essential to characterize the respective tensors in their proper chemical environment [3,51].

The main tensor elements of the ^{15}N chemical shift tensor of the amide bond have approximate values of 61, 75 and 223 ppm (σ_{11}, σ_{22}, σ_{33}). In α-helical peptides the σ_{11} and σ_{33} components are oriented within the plane of the peptide bond, and the NH vector and the σ_{33} component cover an angle of about 18° [13]. By inspecting a molecular model of an α-helix, it becomes obvious that both are oriented within a few degrees along the helix long axis (Fig. 2F).

Fig. 4 shows simulations of ^{15}N solid-state NMR obtained from a model for α-helical polypeptides reconstituted into oriented membranes with the membrane normal parallel to the magnetic field direction. In order to prepare this figure the spectra from helices with different tilt angles were calculated. To create the simulated spectra, all backbone atoms of the 18-residue helices were considered to be labeled with ^{15}N, the resulting spectral line shapes thus represent the addition of individual lines from all these sites. The exact alignment of the peptide bond (e.g. as viewed by its NH vector) with respect to the magnetic field direction (B_o), and thus the measured ^{15}N chemical shift is a function of both the tilt angle (δ) and the rotational pitch angle (γ, Fig. 2F). In the special case of a regular helix adopting a perfect transmembrane alignment, all NH vectors exhibit an identical alignment with respect to the membrane normal and, therefore, also to B_o. Inspection of Fig. 4 indicates, that in general, a given ^{15}N chemical shift can agree with a set of tilt and rotational pitch angles, and does not provide a unique solution. For example, a value of 200 ppm is in agreement

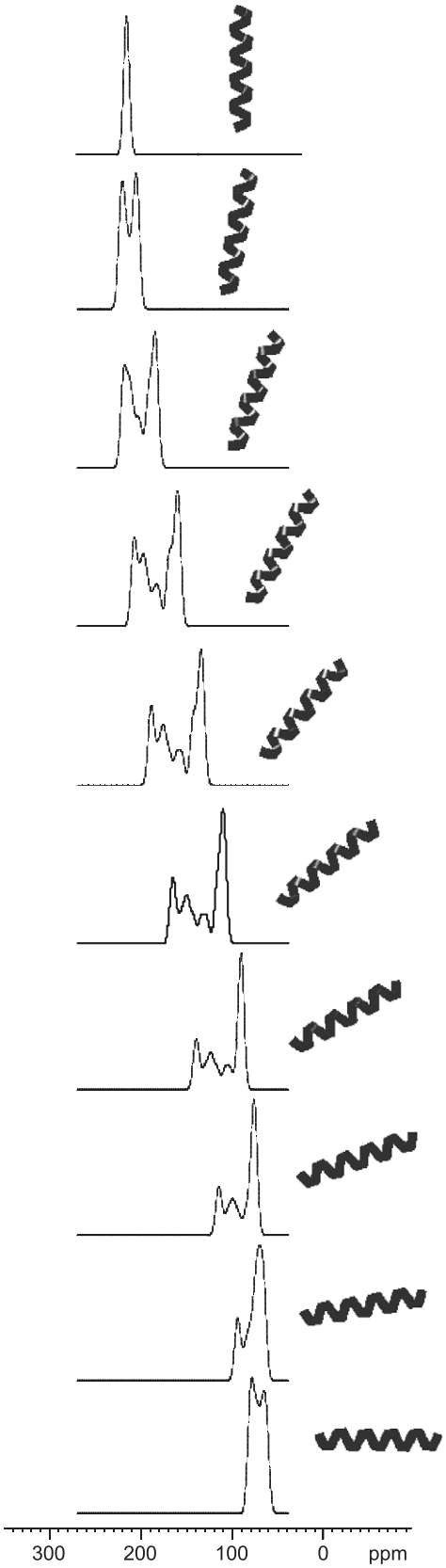

Fig. 4. Simulations of proton-decoupled ^{15}N chemical shift spectra of helices oriented with their long axes at the angles indicated. The sum of the spectra from the individual amide sites is shown a single site label will, therefore, be found within the anisotropic chemical shift dispersion indicated. During the simulations, the static main tensor elements were 223, 75 and 61 ppm with an alignment of the tensor elements within the molecular frame as described in Refs. [51,78].

with tilt angles in the 10° to 30° range (Fig. 4). However, the ^{15}N chemical shift measurement restricts the possible tilt angles. Therefore, in samples uniaxially oriented with the membrane normal parallel to the magnetic field transmembrane α-helical peptides with a tilt angle ≤20° exhibit ^{15}N resonances >180 ppm (Fig. 4). In contrast, ^{15}N chemical shifts <100 ppm are observed when helices are aligned approximately parallel to the membrane surface.

4. Motional averaging

So far the helix has been assumed completely immobilized on the NMR time scale. In a next step, the dynamic properties within the membranes shall be taken into consideration.

In liquid crystalline membranes, rotational diffusion around the membrane normal occurs. Fast continuous diffusion results in partial averaging of the chemical shift anisotropy, which is thus described by an axially symmetric tensor. Its unique component parallel to the rotation axis is $\sigma_{||}$. The two identical components perpendicular to this axis are labeled $\sigma_{\perp}$ (Fig. 2C and F). The new averaged tensor elements are a function of the Euler angles α and β connecting the rotation axis and the static tensor elements (Fig. 2G):

$$\sigma_{||} = \sigma_{11}\cos^2\alpha\sin^2\beta + \sigma_{22}\sin^2\alpha\sin^2\beta + \sigma_{33}\cos^2\beta \quad (5)$$

$$\sigma_{\perp} = \frac{1}{2}\left[\sigma_{11}\left(1-\cos^2\alpha\sin^2\beta\right) + \sigma_{22}\left(1-\sin^2\alpha\sin^2\beta\right) + \sigma_{33}\sin^2\beta\right]. \quad (6)$$

In case of membrane samples oriented with their normal parallel to the magnetic field directions $\sigma_{||}$ and the measurable σ_{zz} coincide. When the Euler angle α corresponds to rotations of the PAS around (σ_{33}), β is, at first approximation, a measure of the helix tilt angle δ (Fig. 2F). From Eqs. (5) and (6) it can be shown that

$$\sigma_{||} = (\sigma_{33} - \sigma_{xx})\cos^2\beta + \sigma_{xx}. \quad (7)$$

Depending on the choice of α, σ_{xx} assumes values between σ_{11} and σ_{22} [13]. When keeping with the above assumptions, i.e. the small difference between the alignment of σ_{33} and the helix long axis are ignored and rotational averaging predominantly occurs around an axis parallel to the magnetic field direction/bilayer normal, the measured ^{15}N chemical shift ($\sigma_{||}$) can thus be used as a direct indicator of the helix tilt angle [13].

In membranes that are uniaxially oriented with the normal parallel to the magnetic field direction (B_o) rotational diffusion around the normal does not change the peptide alignment relative to B_o. However, other modes of motion are also present and should not be ignored. When considering the polypeptide backbone, these include averaging around the helix long axis, wobbling and librational motions, or conformational changes.

Additional degrees of freedom exist when the peptide side chains are considered [53–57]. Such motions result in a directed scaling of the chemical shift and dipolar anisotropies (Fig. 2C and F). When the goal is to obtain accurate angular restraints, these have to be considered independently for every labeled site.

In an analogous manner the ^2H quadrupolar splitting is also strongly dependent on the alignment of the molecule relative to the magnetic field direction. Fig. 3A, B shows ^2H NMR spectra of a model peptide labeled with $^2H_3$-alanine and reconstituted into oriented phospholipid bilayers. Due to fast rotation around the C_α–C_β bond the three labeled sites are equivalent and a single quadrupolar splitting is observed. The C_α atom being an integral part of the protein backbone the orientation-dependent deuterium quadrupole splitting provides an additional restraint, which allows one to better orient the α-helical peptide relative to the membrane normal. The measured splitting $\Delta\nu_Q$ is directly related to the orientation of the C_α–C_β bond:

$$\Delta\nu_Q = \frac{3}{2}\frac{e^2qQ}{h}\frac{(3\cos^2\Theta - 1)}{2}. \quad (8)$$

Here Θ is the angle between C_α–C_β bond and the magnetic field direction and $\frac{e^2qQ}{h}$ the static quadrupolar coupling constant [58]. For example, at room temperature the deuterium quadrupole splitting of a methyl-deuterated alanine exhibits quadrupolar splittings ≤80 kHz.

The contour plots shown in Fig. 5 map the tilt and rotational pitch angles of this peptide that are in agreement with the experimental ^{15}N chemical shift and the ^2H quadrupolar splittings of the labeled sites. The regions of

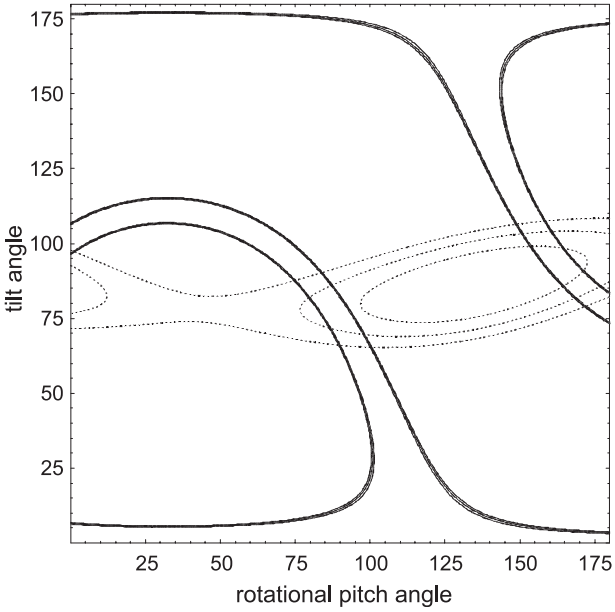

Fig. 5. Map of alignments of LK15 reconstituted in oriented C20-PC. The contours indicate helix orientations where the tilt and the rotational pitch angle agree with the ^{15}N chemical shift (hatched lines, Fig. 2A) and the deuterium quadrupole splitting (continuous lines, Fig. 3A).

overlap are those peptide alignments that are in agreement with both measurements.

In non- or partially oriented samples the signals of individual molecules add up. The resulting line shape is a function of the orientational distribution of the labeled sites. When all orientations have equal probability 'powder pattern' line shapes are obtained (Fig. 2D). For example, the chemical shift powder-pattern is determined by the functional relationship between the chemical shift and molecular orientation (Eqs. (3) or (5)) and the number of molecules at a given orientation relative to the magnetic field direction. Whereas a static powder pattern line shape is shown in Fig. 2D, a motionally averaged line shape is represented in Fig. 2C. Clearly, these powder pattern spectra are indicators not only of the anisotropic chemical shift dispersion but they are also very sensitive to the rate, direction and mechanism of intra- and intermolecular exchange processes including motional averaging [51,59,60]. As illustrated in Fig. 2C and F, averaging around a 'unique' axis results in 'symmetric powder patterns', which are characterized by discontinuities at $\sigma_{\parallel}$ and $\sigma_{\perp}$. The simulations and experimental spectra shown in Fig. 2 indicate that under conditions where the membrane normal coincides with this unique axis of averaging, the powder pattern line shape can be used to extract the tilt angle of the peptide helix [13]. When peptides have been investigated, these averaging effects have often been ignored, although this effect has long ago been described for the ^{31}P chemical shift or the ^{2}H solid-state NMR spectra of phospholipid bilayers [61].

In liquid crystalline bilayers, the ^{31}P chemical shift spectra of phosphatidylcholines are characterized by a symmetric tensor where the tensor singular axis ($\sigma_{\parallel}$) coincides with the rotational axis [62]. The signal at 30 ppm is thus indicative of phosphatidylcholine molecules with their long axis oriented parallel to the magnetic field direction, whereas a −15 ppm ^{31}P chemical shift is obtained for perpendicular alignments. In perfectly aligned samples, the phospholipid bilayer spectra consist of a single line. Tilting the sample in a stepwise manner results in values between these extremes [62].

This effect is routinely used in our laboratory to control the degree of sample alignment when samples have been applied onto planar cover glasses [6]. At sample orientations with the normal parallel to the magnetic field direction, intensities to the right of this 30 ppm peak can arise from phospholipids with molecular orientations deviating from parallel to the magnetic field direction. However, it should be noted that signals in this region (<30 ppm) can also be due to local conformational changes of the phospholipid head group. These include, for example, electrostatic interactions of the ($-HPO_4^-$–CH_2–CH_2–$N^+(CH_3)_3$) dipoles of the phosphocholine head group, hydrogen bonding, and/or electric dipole–dipole interactions [63–65]. Therefore, a single line should be observed for an 'oriented sample' if the phosphatidylcholine molecules, or more precisely, the head group region around the phosphate atoms, adopt the same conformation and are all aligned in the same direction.

5. Dipolar couplings

The dipolar coupling between two nuclei is another important interaction that exerts a strong influence on the appearance of solid-state NMR spectra. In an analogous manner the orientation-dependence of this interaction has also been used to derive structural information for membrane-associated polypeptides (reviewed in e.g. Refs. [3,4,6]). The dipolar interaction between two spins I and S is a function of the gyromagnetic ratios γ_1 and γ_2 of both nuclei, as well as the internuclear distance r, and the angle θ of this vector $\boldsymbol{r}$ with respect to the magnetic field direction. The dipolar interaction term shifts the Zeeman transitions by $+\omega_D$ and $-\omega_D$, thereby resulting in dipolar splitting of [18,66,67]:

$$D_{zz} = \left(\frac{\mu_0}{4\pi}\right)\frac{\gamma_1\gamma_2\hbar}{r^3}\left(3\cos^2\theta - 1\right) \quad (9)$$

with $\hbar$ being Planck's constant. In a static sample the dipolar interaction between ^{15}N and ^{1}H within an amide bond is in the range -20 kHz $\leq\Delta\nu\leq$10 kHz. Such heteronuclear dipolar couplings are also essential during the often applied solid-state NMR cross-polarization experiments [68], where magnetization is transferred from nuclei with high magnetogyric ratio γ, such as ^{1}H, to low-γ nuclei (e.g. ^{13}C or ^{15}N). In liquid crystalline membranes these dipolar couplings are often partially averaged by molecular motion resulting in a reduced transfer efficiency (e.g. Ref. [69]).

6. Solid-state NMR spectra of oriented samples at different tilt angles

The solid-state NMR spectroscopic investigation of peptides reconstituted into oriented membranes allows for the detailed analysis not only of the structural and topological properties but also of the dynamics at the site of the isotopic label. In principle, the oriented samples can be measured at many different alignments. Indeed tilt series or at least two different tilt angles have previously been studied during the investigation of melittin using ^{13}C- [70], the Influenza M2 sequence using ^{15}N- [71], or the labeled retinal moiety in bacteriorhodopsin using deuterium solid-state NMR spectroscopy [72]. However, for structural studies, the investigation of well-aligned membranes with the bilayer normal parallel to the magnetic field direction is generally preferred [3,6]. In this latter set-up, rotational diffusion around the membrane normal does not change the alignment of the peptide relative to the magnetic field direction. The line width observed for chemical shift or dipolar interaction spectra is in this case affected by the mosaic spread of the sample, which represents the range of deviations from a unique alignment of molecules with

respect to the magnetic field direction. In general, a Gaussian distribution function is assumed. Line broadening also arises due to conformational heterogeneity, the dynamic interchange between different membrane topologies, residual dipolar couplings or enhanced relaxation. In order to avoid line broadening effects due to interactions between neighboring spins, decoupling techniques have proven to significantly ameliorate the spectral resolution [17,73–75].

On the other hand the line shapes observed in solid-state NMR spectra of samples oriented with the membrane normal perpendicular to the magnetic field direction are strongly dependent on the rotational diffusion constant in bilayer environments. This sample set-up therefore has its own merits. In the 'perpendicular orientation' free rotation around the membrane normal results in different orientations of the molecules with respect to magnetic field direction (B_o). A priori one would expect broad line shapes representing the distribution of molecular alignments along a circle [12]. Therefore, in case of slow diffusion rates each peptide alignments will be characterized by its own separate signal intensity. If, however, the diffusion rate exceeds the spectral anisotropy averaging is observed. For an object of cross-sectional area A in an environment of viscosity η, the rotational diffusion coefficient D_{pep} at temperature T is given by:

$$D_{pep} = \frac{k_B T F}{4Ah\eta}. \quad (10)$$

In this equation k_B is the Boltzmann constant, h the thickness of the membrane and F the shape factor for non-spherical objects [76,77]. The radius of the molecule relative to the membrane normal a, and its shape factor provides a crude model to estimate the frequency of rotational diffusion of a molecule associated with a lipid bilayer.

In our laboratory, we have been able to obtain ^{2}H and ^{15}N solid-state NMR spectra of model peptides that exhibit mosaic spreads in the 1° range (Figs. 2 and 3). The peptides studied include a transmembrane and several in-plane oriented sequences of different length [78]. When the samples containing short ^{2}H-labeled peptides are tilted from membrane alignments with the normal parallel to the membrane to perpendicular orientations the quadrupolar splitting is reduced to half the size (Fig. 3A and B). This observation is in excellent agreement with theoretical considerations [61]. In an analogous manner, the ^{15}N chemical shift signal retains its Lorentzian-like lineshape (Fig. 2A,B) although its values shift according to the new average orientation of the molecule relative to B_o [13].

Deuterium solid-state NMR spectra of peptides associated with membranes oriented with the normal perpendicular to the magnetic field have also been obtained using bicelles that under certain conditions magnetically orient with the magnetic field of the spectrometer. Using these systems oriented and non-oriented membrane systems are obtained and the structure and orientation of mastoparan X [79], prion protein 130–136 [80], or the TM domain of the Neu tyrosine kinase receptor [81] investigated in bilayer environments.

When the rotational diffusion of the peptides is reduced the sharp peak intensities are lost upon tilting and powder-type line shapes are observed. Using these molecules it was possible to show that indeed the quadrupolar line shape of a $^2H_3$-alanine labeled peptides is much more sensitive to the length of the corresponding α-helix and the phase properties of the membranes when compared to the proton-decoupled ^{15}N spectra [78]. This is in perfect agreement with our estimates, which predict that at viscosity constants, η, that have been established for phospholipid bilayers, the quadrupolar anisotropy of the alanine methyl group (70 kHz) is sensitive to small changes in peptide geometry whereas averaging of the ^{15}N chemical shift anisotropy (7 kHz at 9.4 T) occurs for much larger polypeptide assemblies. The ^{2}H solid-state NMR approach is thus sensitive to monomer–multimer transitions of transmembrane helical peptides, whereas much larger aggregates have to form to significantly change the appearance of the ^{15}N chemical shift spectra [78b].

7. Magic angle spinning NMR spectroscopy (MAS and MAOSS)

Similar to what has been shown for dipolar interactions, the NMR interactions in the solid-state exhibit angular dependences which are expressed by polynomials of the type (3 $\cos^2\theta - 1$) [17,18,82]. Therefore, the anisotropy of dipolar and chemical shift terms cancel when fast motional averaging occurs by isotropic diffusion (e.g. in solution), or when the sample is mechanically rotated at high speeds around the 'magic angle' (θ_m=54,7°). Therefore, when polycrystalline samples or large biomolecular aggregates are spun at high angular speeds around the magic angle solid-state NMR spectra similar to those obtained from isotropic solutions are obtained (Fig. 1C). Magic angle sample spinning (MAS) was the first technique used to obtain highly resolved NMR spectra of polycrystalline solid samples [26].

Fig. 1B and C shows an MAS spectra of (U–^{13}C, U–^{15}N) L-threonine. The MAS spectrum consists of a central band at the isotropic chemical shift and a set of spinning side bands spaced at integers of $\omega_r/2\pi$ [83–85]. If the spinning speed exceeds the chemical shift anisotropy only the highly resolved central band remains (Fig. 1C) [86]. The spinning side bands provide information about the powder pattern envelope (Fig. 1B) and thus the main tensor elements [83]. In the case of networks of homonuclear dipolar interactions (homogeneous interactions), different spin packets are coupled to each other and sharp lines are only obtained if the spinning speed exceeds the interaction size. In contrast, narrowing can already be achieved even if this condition is not matched for non-homogeneous interactions such as the

chemical shift anisotropy or the quadrupolar and heteronuclear dipolar interactions [18,84,85].

Notably, the spinning side band pattern is indicative of the distribution of orientations in the sample. A sample which is rotated at low spinning speed and where all orientations are equally distributed yields a spinning side band structure with an envelope corresponding to the powder pattern line shape of the static spectrum (Figs. 1B and 6B). When MAS is applied to oriented samples (magic angle-oriented sample spinning, MAOSS), the spinning side band intensities are sensitive to partial or complete ordering within the samples [87]. This is obvious when comparing the spectra shown in Fig. 6B and C. The side band intensities of the latter are indicative of an orientation of the lipid long axis perpendicular to the spinning axis (Fig. 6C). When compared to the side band obtained from a randomly oriented sample (Fig. 6B) it becomes obvious that every second side band is missing. The pronounced difference makes slow spinning MAS NMR a useful technique to investigate the alignment and membrane interactions of phospholipids, peptides or proteins within oriented bilayer samples [87,88]. Due to the suppression by the support of membrane undulations that occur on a slow time scale, the spectral line width of these samples is considerably reduced and resolution concomitantly improved [87]. The oriented bilayers have been prepared on glass plates (Fig. 6F) [87] or on extended plastic foils (Fig. 6E) [88]. The plastic polymer is bendable and can be wrapped into cylinders that fit into 4 or 7 mm rotors. Both geometries maintain the cylindrical symmetry around the rotor axis. The set-up shown in Fig. 6E results in alignments of the membrane normal parallel to the spinning axis.

Whereas the ^{31}P MAOSS NMR spectra provides good indication of the quality of membrane alignment using either sample set-up [87] ^{15}N, ^{13}C and ^{2}H MAOSS solid-state NMR spectroscopy has been used to study the alignment of polypeptides or protein prosthetic groups within bilayers [88–91]. Recently, MAOSS solid-state NMR spectroscopy was applied to bacteriorhodopsin selectively labeled with ^{15}N-methionin [92]. This approach allowed to resolve several sites and to analyze their alignment relative to the membrane normal. Notably, both the ^{15}N chemical shift MAOSS NMR spectrum and the ^{13}C–^{15}N REDOR decay curves (i.e. dipolar interaction) are sensitive to the tilt angle of the ^{15}N (and ^{13}C) labeled α-helical peptides [91]. When compared to the original set-up using round glass plates (Fig. 6F; [87]) the spiral geometry is less accurate in determining the exact alignment of in-plane oriented helices. However, the latter arrangement supports the phospholipid bilayers in the direction of the centrifugal forces thereby allowing for much higher spinning speeds (Fig. 6D and E; [88]). Both experimental

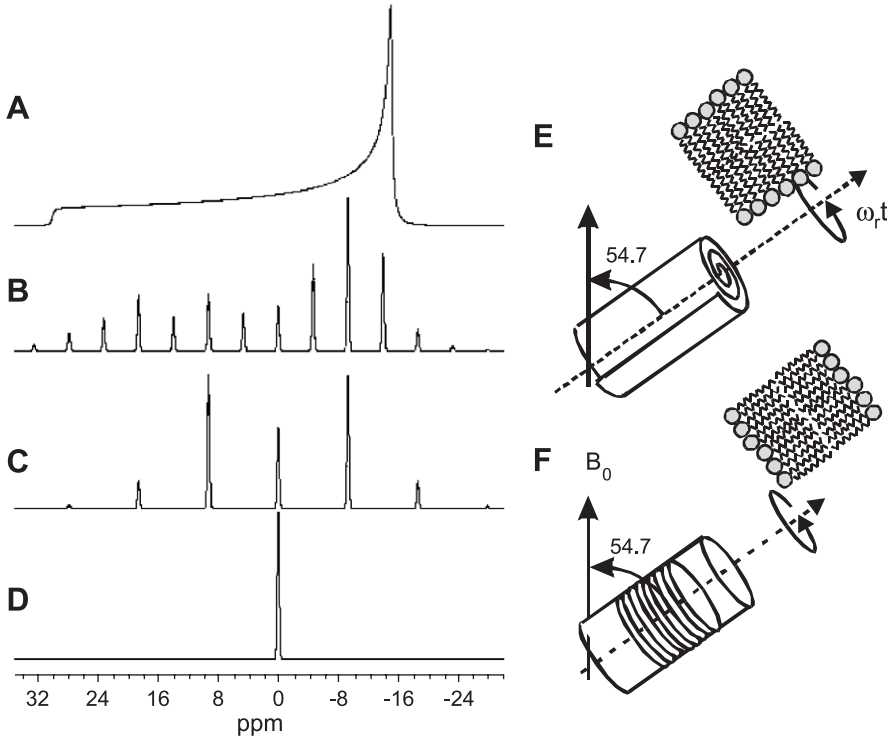

Fig. 6. Simulated proton-decoupled ^{31}P MAS solid-state NMR spectra of hydrated phosphatidylcholine liquid crystalline bilayers at a resonance frequency of 162 MHz, using $\sigma_{\parallel}$=30 and $\sigma_{\perp}$=−15 ppm. (A) Powder sample under static conditions. (B) Non-oriented sample at 750 Hz spinning frequency. (C) Bilayer oriented in a perfect manner along a polymer cylinder with the membrane normal perpendicular to the rotor axis (panel E) at 750 Hz spinning frequency. (D) Bilayer oriented with the membrane normal parallel to the rotor axis (panel F) at 750 Hz spinning frequency. The same isotropic line shape is obtained when a powdered sample is spun at 10 kHz spinning speed. (E) The sample set-up using oriented membranes on rolled cylinders of a polymer sheet. The cylinder can be inserted into 4 or 7 mm MAS rotors [88]. (F) Uniaxial geometry of membranes applied to stacked glass cover slips and inserted into a 7 mm (o.d.) rotor [87].

set-ups combine the advantages of static oriented solid-state NMR spectroscopy with high-resolution MAS NMR spectroscopy.

A related approach was chosen when peptides were associated with bicelles. These disc-shaped structures are known to orient within the magnetic field [93,94]. The director axis of these systems can be manipulated by spinning the sample which extends the field of applications of these macroscopic structures [95]. In a most recent application, bicelles were used for the solid-state NMR investigation of the 35-residue transmembrane region of the tyrosine kinase receptor Neu and the pentapeptide methionine-enkephalin [81].

8. Examples of structural investigations of polypeptides by solid-state NMR

During the last few years solid-state NMR spectroscopy has been applied to a multitude of polypeptides that have been labeled with ^{15}N, ^{13}C and/or ^{2}H and reconstituted into oriented lipid bilayers. Often these polypeptides exhibit a preference for α-helical conformations and the secondary structure in membrane environments is already known from other spectroscopic techniques such as CD, FTIR, Raman, or solution NMR spectroscopy. The anisotropic ^{15}N chemical shift can then be used directly to obtain information about the helix orientation with respect to the bilayer normal (Figs. 4 and 5).

If this information is lacking or needs to be confirmed in more detail in bilayer environments, the investigation of additional interactions of nuclei within the peptide bond allows for a detailed analysis of the peptide secondary structure. The technique has proven its potential during the pioneering work of Ketchem et al. [96] who have used oriented solid-state NMR spectroscopy to describe in detail the high-resolution structure of the *Bacillus brevis* peptide gramicidin A when reconstituted in phospholipid bilayers. This channel peptide assumes a transmembrane right-handed β-helix with 6.3 residues per turn when reconstituted into membranes. This unusual polypeptide conformation is the result of alternating L- and D-amino acids in the gramicidin A sequence. In contrast, the solid-state NMR structural data measured for the magainin 2 antibiotic peptide are only in agreement with a right-handed α-helix oriented parallel to the membrane surface [97].

Vpu is a small accessory protein of 81 amino acids that fulfills important functions during the life cycle of the human immunodeficiency virus 1 [98,99]. Early on the hydrophobic channel-forming domain of Vpu has been synthesized and labeled with ^{15}N isotope labels incorporated individually at positions 10, 14, or 18. After reconstitution of these peptides into oriented phospholipid bilayers, all three labeled positions exhibit resonances between 210 and 220 ppm when investigated by proton-decoupled ^{15}N solid-state NMR spectroscopy [100]. These values are indicative of residues that are part of transmembrane helices (Fig. 4). The experiments were designed to test if the helix–loop–helix structure observed in TFE/water solutions also persists in membrane environments [100]. A quantitative analysis of the solid-state NMR data indicates that this is not the case. However, when taking into consideration potential sources of error, including the precision of experimental data and the description of the underlying tensors elements, a continuous right-handed α-helix, with tilt angles of $20\pm10^{\circ}$ agrees well with the solid-state NMR data. Transmembrane helix alignments were also found using ATR FTIR measurements [101] and solid-state experiments on perlabeled samples [102].

When the transmembrane region of the related M2 polypeptide of Influenza A has been investigated by solid-state NMR spectroscopy the ^{15}N chemical shifts recorded from five isoleucine and two valine residues within the sequence are in agreement with a uniform transmembrane helix at a tilt angle of $35\pm3^{\circ}$ [71,103,104]. Model building indicates, that, in order for a polar water-filled cavity to be formed within a four-helix bundle, the twist of such a pore needs to be left-handed [105]. Interestingly, this angle differs significantly from tilt angle of approximately 25° measured for the full-length proton channel [106]. The ^{15}N solid-state NMR spectra of oriented M2 transmembrane sequence in the presence of the antiviral drug amantadine do not show profound changes of the alignment of the polypeptide [6,107]. Other examples of transmembrane channel peptides investigated by oriented ^{15}N solid-state NMR spectroscopy include the fungal peptide alamethicin [32,108,109], or the putative channel-lining sequence M2 of the acetyl choline receptor [110,111].

Amphipathic peptide antibiotics are found in many species including amphibians [112–114], insects [115] or humans [116]. Magainins from frogs and cecropins from insects have indeed been shown to adopt α-helical secondary structures in membrane environments using a wide variety of biophysical methods and this has been reviewed in considerable detail in an earlier BBA issue [117]. Oriented solid-state NMR spectroscopy indicates that at concentrations ≤3% (mol/mol) these and related peptides orient parallel to the membrane interface suggesting detergent-like rather than transmembrane channels [117]. However, depending on the detailed composition and environmental parameters of the membranes many different membrane phases, including bilayers, porous bilayers, bicelles and micelles seem possible [6]. A more complete description of the peptide–membrane interactions should thus be based on a phase diagram analogous to those established for detergents or other amphiphile mixtures [118].

The alignment of many other peptides has been investigated using oriented solid-state NMR spectroscopy. These include, just to mention a few of the more recent studies, a fusion peptide from sea urchin by ^{19}F NMR [119], protegrin 1 by ^{13}C NMR [120], or antibiotic peptides from Australian tree frogs [121].

The interaction contributions that determine the peptide topology and the association within the membrane have been studied by oriented solid-state NMR spectroscopy. To this purpose a large number of hydrophobic and amphipathic helical peptides were synthesized, reconstituted into non-oriented or oriented bilayers and investigated in a quantitative manner using ^{2}H, ^{31}P-[122–124] or ^{15}N chemical shift solid-state NMR [28,125–127] as well as AT-FTIR spectroscopy [128,129]. Interestingly, amphipathic model peptides have not only been shown to be highly potent antibiotics, but they also act as DNA vectors [130,131]. When the orientation of these histidine-rich peptides is measured as a function of pH, a transition is observed between transmembrane and in-plane orientations for many of these sequences [28,78,132]. A thermodynamic analysis of the Gibbs free energy that governs the membrane alignment of helical peptides needs to include hydrophobic interactions, the energy required to discharge an amino acid side chain at a given pH, the energy of placing a polar side chains in the hydrophobic membrane interior as well as hydrophobic mismatch contributions [28,78,126]. In this context the role of histidine, lysine, alanine, and leucine side chains has been investigated in considerable detail [132].

9. Magic angle sample spinning solid-state NMR spectroscopy

MAS results in averaging of the anisotropy of dipolar, quadrupolar and chemical shift interactions [26,83,85,133–135]. At the same time, residual heteronuclear interactions with ^{1}H are suppressed by high-power proton irradiation. Using these two methods, well-resolved NMR spectra are obtained, in which the resolution of resonances is to a large extent determined by the sample heterogeneity [136]. This technique has also been extensively applied to biomolecules in precipitates, fibrils, aggregates, membranes or in other states where re-orientational diffusion is reduced (recent reviews, e.g. Refs. [10,137]). The resulting solid-state NMR spectra provide ^{15}N and ^{13}C chemical shifts, which are useful indicators of polypeptide main chain conformation [138]. In particular, the analysis of the C_{α} and C_{β} chemical shifts shows that these correlate with backbone torsion angles of proteins in solution [139,140] and in the solid-state [141–144]. Whereas MAS averages or completely eliminates the dipolar interaction terms NMR pulse sequences have been developed for their selective reintroduction. Such pulse sequences thereby allow to accurately determine distances (reviewed in Refs. [4,6,145–149]) or dihedral angles between nuclei when at the same time high resolution NMR spectra are maintained in the chemical shift domain [150–158]. Recent examples include measurements of the ligand-induced conformational change in a bacterial serine chemoreceptor [159], an interhelical distance in the closed state of the Influenza A M2 proton channel [160], distances within the glycophorin dimer interface [161], conformational studies of a ternary enzyme complex [162], or measurements on rhodopsin [163,164], the HIV fusion peptide [165], phospholamban [166], melittin [141,167] and the Neu receptor tyrosine kinase [168]. These MAS dipolar recoupling methods have been extended to applications to selectively [31,169] or uniformly labeled sequences within polypeptides thereby reducing the number of the peptides that need to be prepared for such studies [170–176].

Furthermore, recent years have seen some exciting developments in the application of MAS solid-state NMR spectroscopy at the highest magnetic fields currently available. This has resulted in the assignment and structure determination of uniformly labeled polypeptides. Methods analogous to those routinely used in solution NMR spectroscopy have been developed and applied to some, albeit still comparatively small, model proteins in the solid-state [177]. This has, for example, resulted in the solid-state NMR structure of the 62-residue SH3 domain in its crystalline form [14]. During this investigation, substantial efforts initially went into the search of optimal sample conditions [136]. Thereafter methods for the assignment of most ^{13}C and ^{15}N resonances have been developed and applied [178–180]. These assignment experiments exploit dipolar and scalar interactions between close-by and bonded nuclei [178,181–187]. For assignment purposes homo- or heteronuclear correlation experiments have been established which use magnetization transfer schemes such as proton-driven spin diffusion (PDSD) [178,184,188] or radiofrequency recoupling schemes. The latter include cross-polarization [184], MELODRAMA [189], SPECIFIC CP [178], C7 [190], DQF Post-C7 [188,191,192], RFDR [186], or DREAM [178,193]. For example, the 'spectrally induced filtering in combination with cross-polarization' (SPECIFIC CP) sequence is used to selective transfer magnetization from one type of nucleus (such as ^{15}N) to a selected frequency band of another nucleus (e.g. ^{13}C) [194]. An important advantage of this technique is that it does not require excessively high radiofrequency fields, thereby avoiding detrimental effects on the sample. Another route uses dipolar filtering to suppress directly bonded C–H correlations thereby simplifying the ^{1}H–^{13}C heteronuclear correlation spectra [195].

In a last step, inter-residue distance information has been collected for the SH3 protein [14]. To this purpose ^{1}H–^{1}H contacts need to be established which is difficult due to the strong couplings between these abundant nuclei. The problems can be overcome using elaborate isotopic labeling schemes, which dilute the ^{1}H density by ^{2}H [191,196], or by ^{13}C block labeling strategies [14,33,197]. By removing the ^{1}H–^{1}H and ^{13}C–^{13}C interactions between nearest neighbors the problem of detecting non-trivial structural constraints if simplified. More recently, methods have been developed that allow to establish ^{1}H–^{1}H contacts in the solid-state

indirectly through encoding in CHHC or NHHC correlation schemes [188,192,198]. During the last few years, there has also been increasing interest in the direct detection of the ^{1}H nuclei, which is more sensitive than recording the precessions of ^{13}C or ^{15}N. However, due to the strong interactions between the protons this is only possible for small sample volumes which allow spinning speeds >30 kHz [199–201], or alternatively when the ^{1}H spins have been diluted by deuterons [196].

Other related examples include structural studies of ubiquitin [184,185], BPTI [186], the dimeric form of the 10.4 kDa *B. subtilis* protein Crh [202,203], or amyloid fibrils [173,204,205]. Unfortunately, the applications of these techniques to membrane proteins seems to be more difficult as these proteins are either considerable bigger or they show unfavorable dynamic properties which result in broadened line shapes. Notably, the advantages of crystalline samples have been recognized early on but this strategy was rejected as 'not meaningful for non-crystalline and disordered proteins' [185]. Instead, this author developed a novel three-dimensional experiment for assignment purposes thereby considerably improving resolution. Despite the particular problems associated with membrane proteins, some very interesting results have been obtained when applying the novel pulse sequences shortly described in the above paragraph to bacteriorhodopsin [187,206], or the retinal moiety in rhodopsin [207]. Interestingly, several residues of the transmembrane helices of the LH2 light-harvesting complex could be resolved and assigned, whereas correlation residues involving the N- and C-terminal loop regions were attenuated [208]. Furthermore, a hexapeptide bound to the neurotensin receptor has been investigated [209,210]. Notably, the linear β-strand conformation of the high-affinity agonist to the neurotensin receptor could be derived merely from the chemical shift information, which thus provided a favorable case to an otherwise very ambitious project [210].

Solid-state NMR has opened new avenues to the investigation of immobilized proteins or complexes thereof, including membrane-associated polypeptides. The progress of this technique will be enhanced in the future as more and more scientists recognize its potential and will help in its progress.

Acknowledgments

We are grateful to the *Agence Nationale pour la Recherche contre le SIDA* for financial support in particular to C.A. We acknowledge the help of Josefine März for her help during the initial steps of peptide synthesis and purification, Monika Zobawa for recording mass spectra and Christina Sizun for establishing the MAOSS simulation program. We are grateful to Bas Vogt who performed some initial studies on oriented ^{2}H NMR spectroscopy of peptides in our laboratory.

References

[1] J. Torres, T.J. Stevens, M. Samso, Trends Biochem. Sci. 28 (2003) 137–144.
[2] A. Arora, L.K. Tamm, Curr. Opin. Struct. Biol. 11 (2001) 540–547.
[3] T.A. Cross, Methods Enzymol. 289 (1997) 672–696.
[4] R.G. Griffin, Nat. Struct. Biol., NMR (Suppl. 5) (1998) 508–512.
[5] J.H. Davis, M. Auger, Prog. NMR Spectrosc. 35 (1999) 1–84.
[6] B. Bechinger, R. Kinder, M. Helmle, T.B. Vogt, U. Harzer, S. Schinzel, Biopolymers 51 (1999) 174–190.
[7] A. Watts, Mol. Membr. Biol. 19 (2002) 267–275.
[8] P.T. Williamson, B.H. Meier, A. Watts, Eur. Biophys. J. 33 (2004) 247–254.
[9] A. Drechsler, F. Separovic, IUBMB Life 55 (2003) 515–523.
[10] S. Luca, H. Heise, M. Baldus, Acc. Chem. Res. 36 (2003) 858–865.
[11] A. Watts, Curr. Opin. Biotechnol. 10 (1999) 48–53.
[12] B. Bechinger, Phys. Chem. Chem. Phys. 2 (2000) 4569–4573.
[13] B. Bechinger, C. Sizun, Concepts Magn. Reson. 18A (2003) 130–145.
[14] F. Castellani, B. van Rossum, A. Diehl, M. Schubert, K. Rehbein, H. Oschkinat, Nature 420 (2002) 98–102.
[15] K. Wüthrich, NMR of Proteins and Nucleic Acids, John Wiley & Sons, New York, 1986.
[16] J. Cavanagh, W.J. Fairbrother, A.G. Palmer III, N.J. Skelton, Protein NMR Spectroscopy, Principles and Practice, Academic Press, San Diego, 1996.
[17] U. Haeberlen, High Resolution NMR in Solids, Selective Averaging, Academic Press, New York, 1976.
[18] M. Mehring, Principles of High Resolution NMR in Solids, Springer, Berlin, 1983.
[19] T.A. Cross, J.R. Quine, Concepts Magn. Reson. 12 (2000) 55–70.
[20] R.G. Griffin, Methods Enzymol. 72 (1981) 108–173.
[21] J.M. Griffiths, T.T. Ashburn, M. Auger, P.R. Costa, R.G. Griffin, P.T. Lansbury, J. Am. Chem. Soc. 117 (1995) 3539–3546.
[22] R. Tycko, Biochemistry 42 (2003) 3151–3159.
[23] M. Bokvist, F. Lindstrom, A. Watts, G. Grobner, J. Mol. Biol. 335 (2004) 1039–1049.
[24] A. Naito, M. Kamihira, R. Inoue, H. Saito, Magn. Reson. Chem. 42 (2004) 247–257.
[25] O.N. Antzutkin, Magn. Reson. Chem. 42 (2004) 231–246.
[26] E.R. Andrew, A. Bradbury, R.G. Eades, Nature 183 (1959) 1802–1803.
[27] J.J. de Vries, H.J.C. Berendsen, Nature 221 (1969) 1139–1140.
[28] B. Bechinger, J. Mol. Biol. 263 (1996) 768–775.
[29] M.R. Farrar, K.V. Lakshmi, S.O. Smith, R.S. Brown, J. Raap, J. Lugtenburg, R.G. Griffin, J. Herzfeld, Biophys. 65 (1993) 310–315.
[30] J.G. Hu, B.Q. Sun, M. Bizounok, M.E. Hatcher, J.C. Lansing, J. Raap, P.J.E. Verdegem, J. Lugtenburg, R.G. Griffin, J. Herzfeld, Biochemistry 37 (1998) 8088–8096.
[31] M. Helmle, H. Patzelt, W. Gärtner, D. Oesterhelt, B. Bechinger, Biochemistry 39 (2000) 10066–10071.
[32] B. Bechinger, D.A. Skladnev, A. Ogrel, X. Li, N.V. Swischewa, T.V. Ovchinnikova, J.D.J. O'Neil, J. Raap, Biochemistry 40 (2001) 9428–9437.
[33] M. Hong, K. Jakes, J. Biomol. NMR 14 (1999) 71–74.
[34] J.E. Roberts, S. Vega, R.G. Griffin, J. Am. Chem. Soc. 106 (1984) 2506–2512.
[35] J.S. Waugh, Proc. Natl. Acad. Sci. U. S. A. 73 (1976) 1394–1397.
[36] C.H. Wu, A. Ramamoorthy, S.J. Opella, J. Magn. Reson. 109 (1994) 270–272.
[37] Y. Ishii, R. Tycko, J. Am. Chem. Soc. 122 (2000) 1443–1455.
[38] T. Vosegaard, N.C. Nielsen, J. Biomol. NMR 22 (2002) 225–247.
[39] R. Bertram, T. Asbury, F. Fabiola, J.R. Quine, T.A. Cross, M.S. Chapman, J. Magn. Reson. 163 (2003) 300–309.
[40] M.E. Rose, Elementary Theory of Angular Momentum, John Wiley, New York, 1963.

[41] K. Schmidt-Rohr, H.W. Spiess, Multidimensional Solid-State NMR and Polymers, Academic Press, London, 1994.
[42] C.J. Hartzell, M. Whitfield, T.G. Oas, G.P. Drobny, J. Am. Chem. Soc. 109 (1987) 5966–5969.
[43] T.G. Oas, C.J. Hartzell, F.W. Dahlquist, G.P. Drobny, J. Am. Chem. Soc. 109 (1987) 5962–5966.
[44] Q. Teng, T.A. Cross, J. Magn. Reson. 85 (1989) 439–447.
[45] C.H. Wu, A. Ramamoorthy, L.M. Gierasch, S.J. Opella, JACS 117 (1995) 6148–6149.
[46] D.K. Lee, A. Ramamoorthy, Journal of Magnetic Resonance, 133 (1), Academic Press, 1998 (July).
[47] D.K. Lee, J.S. Santos, A. Ramamoorthy, J. Phys. Chem. 103 (1999) 8383–8390.
[48] S.C. Shekar, A. Ramamoorthy, R.J. Wittebort, J. Magn. Reson. 155 (2002) 257–262.
[49] A. Shoji, T. Ozaki, T. Fujito, K. Deguchi, S. Ando, I. Ando, Macromolecules 22 (1989) 2860–2863.
[50] A. Shoji, T. Ozaki, T. Fujito, K. Deguchi, S. Ando, I. Ando, J. Am. Chem. Soc. 112 (1990) 4693–4697.
[51] N.D. Lazo, W. Hu, T.A. Cross, J. Magn. Res. 107 (1995) 43–50.
[52] A. Shoji, T. Ozaki, T. Fujito, K. Deguchi, I. Ando, J. Magoshi, J. Mol. Struct. 441 (1998) 251–266.
[53] R.R. Ketchem, W. Hu, F. Tian, T.A. Cross, Structure 2 (1994) 699–701.
[54] J.A. Killian, M.J. Taylor, R.E. Koeppe, Biochemistry 31 (1992) 11283–11290.
[55] K.-C. Lee, T.A. Cross, Biophys. J. 66 (1994) 1380–1387.
[56] F. Separovic, J. Gehrmann, T. Milne, B.A. Cornell, S.Y. Lin, R. Smith, Biophys. J. 67 (1994) 1495–1500.
[57] W. Hu, N.D. Lazo, T.A. Cross, Biochemistry 34 (1995) 14138–14146.
[58] J. Seelig, Q. Rev. Biophys. 10 (1977) 353–418.
[59] B. Bechinger, M. Zasloff, S.J. Opella, Biophys. J. 74 (1998) 981–987.
[60] D.J. Siminovich, Biochem. Cell. Biol. 78 (1998) 411–422.
[61] J. Seelig, Biochemistry 20 (1981) 3922–3932.
[62] J. Seelig, Biochim. Biophys. Acta 515 (1978) 105–140.
[63] J. Seelig, P.M. Macdonald, P.G. Scherer, Biochemistry 26 (1987) 7535–7541.
[64] B. Bechinger, J. Seelig, Biochemistry 30 (1991) 3923–3929.
[65] B. Bechinger, J. Seelig, Chem. Phys. Lipids 58 (1991) 1–5.
[66] M.H. Levitt, Spin Dynamics, John Wiley & Sons, Chichester, 2001.
[67] J.N.S. Evans, Biomolecular NMR Spectroscopy, Oxford University Press, Oxford, 1995.
[68] A. Pines, M.G. Gibby, J.S. Waugh, J. Chem. Phys. 59 (1973) 569–590.
[69] K.J. Hallock, D.K. Lee, J. Omnaas, H.I. Mosberg, A. Ramamoorthy, Biophys. J. 83 (2002) 1004–1013.
[70] R. Smith, F. Separovic, T.J. Milne, A. Whittaker, F.M. Bennett, B.A. Cornell, A. Makriyannis, J. Mol. Biol. 241 (1994) 456–466.
[71] Z.Y. Song, F.A. Kovacs, J. Wang, J.K. Denny, S.C. Shekar, J.R. Quine, T.A. Cross, Biophysics 79 (2000) 767–775.
[72] A.S. Ulrich, A. Watts, I. Wallat, M.P. Heyn, Biochemistry 33 (1994) 5370–5375.
[73] M. Rance, R.A. Byrd, J. Magn. Res. 52 (1983) 221–240.
[74] A. Bielecki, A.C. Kolbert, H.J.M. de Groot, R.G. Griffin, M.H. Levitt, Adv. Magn. Reson. 14 (1990) 111–124.
[75] D.E. Warschawski, J.D. Gross, R.G. Griffin, J. Chim. Phys. Phys.-Chim. Biol. 95 (1998) 460–466.
[76] R.J. Cherry, Biochim. Biophys. Acta 559 (1979) 289–377.
[77] A.-J. Wang, K.-S. Ho, Chin. Phys. Lett. 19 (2002) 1727–1729.
[78a] C. Aisenbrey, B. Bechinger, Biochemistry 43 (2004) 10502–10512.
[78b] C. Aisenbrey, B. Bechinger, J. Am. Chem. Soc. (2004), in press.
[79] J.A. Whiles, R. Brasseur, K.J. Glover, G. Melacini, E.A. Komives, R.R. Vold, Biophys. J. 80 (2001) 280–293.
[80] K.J. Glover, J.A. Whiles, M.J. Wood, G. Melacini, E.A. Komives, R.R. Vold, Biochemistry 40 (2001) 13137–13142.
[81] C. Sizun, F. Aussenac, A. Grelard, E.J. Dufourc, Magn. Reson. Chem. 42 (2004) 180–186.
[82] D.E. Warschawski, M. Traikia, P.F. Devaux, G. Bodenhausen, Biochimie 80 (1998) 437–450.
[83] J. Herzfeld, A.E. Berger, J. Phys. Chem. 73 (1980) 6021–6030.
[84] E. Lipmaa, M. Alla, T. Tuherm, Proc. Colloq. AMPERE, 19th, Heidelberg, 1976, p. 113.
[85] M.M. Maricq, J.S. Waugh, J. Chem. Phys. 70 (1979) 3300–3316.
[86] E.R. Andrew, A. Bradbury, R.G. Eades, V.T. Wynn, Phys. Lett. 4 (1963) 99–100.
[87] C. Glaubitz, A. Watts, J. Magn. Reson. 130 (1998) 305–316.
[88] C. Sizun, B. Bechinger, J. Am. Chem. Soc. 124 (2002) 1146–1147.
[89] Z. Ahmed, D. Middleton, C. Glaubitz, A. Watts, Biochem. Soc. Trans. 26 (1998) S194.
[90] C. Glaubitz, I.J. Burnett, G. Gröbner, A.J. Mason, A. Watts, J. Am. Chem. Soc. 121 (1999) 5787–5794.
[91] D.A. Middleton, Z. Ahmed, C. Glaubitz, A. Watts, J. Magn. Reson. 147 (2000) 366–370.
[92] A.J. Mason, S.L. Grage, S.K. Straus, C. Glaubitz, A. Watts, Biophys. J. 86 (2004) 1610–1617.
[93] C.R. Sanders II, J.H. Prestegard, Biophys. J. 58 (1990) 447–460.
[94] J.A. Whiles, R. Deems, R.R. Vold, E.A. Dennis, Bioorg. Chem. 30 (2002) 431–442.
[95] G. Zandomeneghi, M. Tomaselli, P.T. Williamson, B.H. Meier, J. Biomol. NMR 25 (2003) 113–123.
[96] R.K. Ketchem, W. Hu, T.A. Cross, Science 261 (1993) 1457–1460.
[97] B. Bechinger, M. Zasloff, S.J. Opella, Protein Sci. 2 (1993) 2077–2084.
[98] R.A. Lamb, L.H. Pinto, Virology 229 (1997) 1–11.
[99] M.E. Gonzalez, L. Carrasco, Biochemistry 37 (1998) 13710–13719.
[100] V. Wray, R. Kinder, T. Federau, P. Henklein, B. Bechinger, U. Schubert, Biochemistry 38 (1999) 5272–5282.
[101] A. Kukol, I.T. Arkin, Biophys. J. 77 (1999) 1594–1601.
[102] S.H. Park, A.A. Mrse, A.A. Nevzorov, M.F. Mesleh, M. Oblatt-Montal, M. Montal, S.J. Opella, J. Mol. Biol. 333 (2003) 409–424.
[103] C. Tian, P.F. Gao, L.H. Pinto, R.A. Lamb, T.A. Cross, Protein Sci. 12 (2003) 2597–2605.
[104] F.A. Kovacs, J.K. Denny, Z. Song, J.R. Quine, T.A. Cross, J. Mol. Biol. 295 (2000) 117–125.
[105] F.A. Kovacs, T.A. Cross, Biophys. J. 73 (1997) 2511–2517.
[106] C. Tian, K. Tobler, R.A. Lamb, L.H. Pinto, T.A. Cross, Biochemistry 41 (2002) 11294–11300.
[107] Z. Song, F.A. Kovacs, J. Wang, J.K. Denny, S.C. Shekar, J.R. Quine, T.A. Cross, Biophys. J. 79 (2000) 767–775.
[108] C.L. North, M. Barranger-Mathys, D.S. Cafiso, Biophys. J. 69 (1995) 2392–2397.
[109] M. Bak, R.P. Bywater, M. Hohwy, J.K. Thomsen, K. Adelhorst, H.J. Jakobsen, O.W. Sorensen, N.C. Nielsen, Biophys. J. 81 (2001) 1684–1698.
[110] B. Bechinger, Y. Kim, L.E. Chirlian, J. Gesell, J.-M. Neumann, M. Montal, J. Tomich, M. Zasloff, S.J. Opella, J. Biomol. NMR 1 (1991) 167–173.
[111] S.J. Opella, F.M. Marassi, J.J. Gesell, A.P. Valente, Y. Kim, M. Oblatt-Montal, M. Montal, Nat. Struct. Biol. 6 (1999) 374–379.
[112] G. Kiss, H. Michl, Toxicon (Oxford) 1 (1962) 33–39.
[113] W. Hoffmann, K. Richter, G. Kreil, EMBO J. 2 (1983) 711–714.
[114] C.L. Bevins, M. Zasloff, Ann. Rev. Biochem. 59 (1990) 395–441.
[115] H.G. Boman, D. Hultmark, Annu. Rev. Microbiol. 41 (1987) 103–126.
[116] R.I. Lehrer, T. Ganz, M.E. Selsted, Cell 64 (1991) 229–230.
[117] B. Bechinger, Biochim. Biophys. Acta 1462 (1999) 157–183.
[118] B. Bechinger, Crit. Rev. Plant Sci. 23 (2004) 271–292.
[119] S. Afonin, U.H. Durr, R.W. Glaser, A.S. Ulrich, Magn. Reson. Chem. 42 (2004) 195–203.
[120] J.J. Buffy, A.J. Waring, R.I. Lehrer, M. Hong, Biochemistry 42 (2003) 13725–13734.
[121] M.S. Balla, J.H. Bowie, F. Separovic, Eur. Biophys. J. 33 (2004) 109–116.

[122] M.R. de Planque, D.V. Greathouse, R.E.2. Koeppe, H. Schafer, D. Marsh, J.A. Killian, Biochemistry 37 (1998) 9333–9345.
[123] M.R. de Planque, J.W. Boots, D.T. Rijkers, R.M. Liskamp, D.V. Greathouse, J.A. Killian, Biochemistry 41 (2002) 8396–8404.
[124] M.R. de Planque, B.B. Bonev, J.A. Demmers, D.V. Greathouse, I.I.R. Koeppe, F. Separovic, A. Watts, J.A. Killian, Biochemistry 42 (2003) 5341–5348.
[125] T.C.B. Vogt, P. Ducarme, S. Schinzel, R. Brasseur, B. Bechinger, Biophys. J. 79 (2000) 2644–2656.
[126] U. Harzer, B. Bechinger, Biochemistry 39 (2000) 13106–13114.
[127] B. Bechinger, Biophys. J. 82 (2001) 2251–2256.
[128] B. Bechinger, J.M. Ruysschaert, E. Goormaghtigh, Biophys. J. 76 (1999) 552–563.
[129] M.R. de Planque, E. Goormaghtigh, D.V. Greathouse, R.E. Koeppe, J.A. Kruijtzer, R.M. Liskamp, B. De Kruijff, J.A. Killian, Biochemistry 40 (2001) 5000–5010.
[130] T.C.B. Vogt, B. Bechinger, J. Biol. Chem. 274 (1999) 29115–29121.
[131] A. Kichler, C. Leborgne, J. März, O. Danos, B. Bechinger, Proc. Natl. Acad. Sci. U. S. A. 100 (2003) 1564–1568.
[132] B. Bechinger, FEBS Lett. 504 (2001) 161–165.
[133] M. Mehring, J.S. Waugh, Phys. Rev., B 9 (1972) 3459–3471.
[134] H. Saito, I. Ando, in: E.A. Webb (Ed.), Ann. Reports on NMR Spect., Academic Press, 1989, pp. 209–290.
[135] A. Watts, Biochim. Biophys. Acta 1376 (1998) 297–318.
[136] J. Pauli, B. van Rossum, H. Forster, H.J. de Groot, H. Oschkinat, J. Magn. Res. 143 (2000) 411–416.
[137] R. Tycko, Annu. Rev. Phys. Chem. 52 (2001) 575–606.
[138] I. Ando, T. Kameda, N. Asakawa, S. Kuroki, H. Kurosu, J. Mol. Struct. 441 (1998) 213–230.
[139] S. Spera, A. Bax, J. Am. Chem. Soc. 113 (1991) 5490–5492.
[140] D.S. Wishart, B.D. Sykes, J. Biomol. NMR 4 (1994) 171–180.
[141] A. Naito, T. Nagao, K. Norisada, T. Mizuno, S. Tuzi, H. Saito, Biophys. J. 78 (2000) 2405–2417.
[142] D. Huster, X. Yao, K. Jakes, M. Hong, Biochim. Biophys. Acta 1561 (2002) 159–170.
[143] S. Luca, D.V. Filippov, J.H. van Boom, H. Oschkinat, H.J. de Groot, M. Baldus, J. Biomol. NMR 20 (2001) 325–331.
[144] H. Saito, S. Yamaguchi, H. Okuda, A. Shiraishi, S. Tuzi, Solid State Nucl. Magn. Reson. 25 (2004) 5–14.
[145] M. Auger, J. Chim. Phys. 92 (1995) 1751–1760.
[146] R. Tycko, Annu. Rev. Phys. Chem. 52 (2001) 575–606.
[147] L.K. Thompson, Curr. Opin. Struct. Biol. 12 (2002) 661–669.
[148] S.O. Smith, K. Aschheim, M. Groesbeek, Q. Rev. Biophys. 29 (1996) 395–449.
[149] L.M. McDowell, J. Schaefer, Curr. Opin. Struct. Biol. 6 (1996) 624–629.
[150] X. Feng, Y.K. Lee, D. Sandström, M. Eden, H. Maisel, A. Sebald, M.H. Levitt, Chem. Phys. Lett. 257 (1996) 314–320.
[151] R. Tycko, D.P. Weliky, A.E. Berger, J. Chem. Phys. 105 (1996) 7915–7930.
[152] J.C. Chan, R. Tycko, J. Am. Chem. Soc. 125 (2003) 11828–11829.
[153] P.T. Williamson, A. Verhoeven, M. Ernst, B.H. Meier, J. Am. Chem. Soc. 125 (2003) 2718–2722.
[154] X. Feng, M. Eden, A. Brinkmann, H. Luthman, L. Eriksson, A. Graslund, O.N. Antzutkin, M.H. Levitt, J. Am. Chem. Soc. 119 (1997) 12006–12007.
[155] P.R. Costa, J.D. Gross, M. Hong, R.G. Griffin, Chem. Phys. Lett. 280 (1997) 95–103.
[156] M. Hong, J.D. Gross, R.G. Griffin, J. Phys. Chem., B 101 (1997) 5869–5874.
[157] B. Reif, M. Hohwy, C.P. Jaroniec, C.M. Rienstra, R.G. Griffin, J. Magn. Reson. 145 (2000) 132–141.
[158] F.J. Blanco, R. Tycko, J. Magn. Res. 149 (2001) 131–138.
[159] B. Isaac, G.J. Gallagher, Y.S. Balazs, L.K. Thompson, Biochemistry 41 (2002) 3025–3036.
[160] K. Nishimura, S. Kim, L. Zhang, T.A. Cross, Biochemistry 41 (2002) 13170–13177.
[161] S.O. Smith, M. Eilers, D. Song, E. Crocker, W. Ying, M. Groesbeek, G. Metz, M. Ziliox, S. Aimoto, Biophys. J. 82 (2002) 2476–2486.
[162] L.M. McDowell, B. Poliks, D.R. Studelska, R.D. O'Connor, D.D. Beusen, J. Schaefer, J. Biomol. NMR 28 (2004) 11–29.
[163] A.F. Creemers, S. Kiihne, P.H. Bovee-Geurts, W.J. deGrip, J. Lugtenburg, H.J. de Groot, Proc. Natl. Acad. Sci. U. S. A. 99 (2002) 9101–9106.
[164] M. Eilers, W. Ying, P.J. Reeves, H.G. Khorana, S.O. Smith, Methods Enzymol. 343 (2002) 212–222.
[165] J. Yang, D.P. Weliky, Biochemistry 42 (2003) 11879–11890.
[166] E. Hughes, D.A. Middleton, J. Biol. Chem. 278 (23) (2003 Jun 6) 20835–20842 (Electronic publication. 2003 Jan 29. 278).
[167] Y.H. Lam, C.J. Morton, F. Separovic, Eur. Biophys. J. 31 (2002) 383–388 (8409413).
[168] S.O. Smith, C. Smith, S. Shekar, O. Peersen, M. Ziliox, S. Aimoto, Biochemistry 41 (2002) 9321–9332.
[169] A.T. Petkova, M. Hatanaka, C.P. Jaroniec, J.G. Hu, M. Belenky, M. Verhoeven, J. Lugtenburg, R.G. Griffin, J. Herzfeld, Biochemistry 41 (2002) 2429–2437.
[170] C.P. Jaroniec, B.A. Tounge, J. Herzfeld, R.G. Griffin, J. Am. Chem. Soc. 123 (2001) 3507–3519.
[171] J. Schaefer, J. Magn. Reson. 137 (1999) 272–275.
[172] V. Ladizhansky, C.P. Jaroniec, A. Diehl, H. Oschkinat, R.G. Griffin, J. Am. Chem. Soc. 125 (2003) 6827–6833.
[173] R. Tycko, Y. Ishii, J. Am. Chem. Soc. 125 (2003) 6606–6607.
[174] E. Crocker, A.B. Patel, M. Eilers, S. Jayaraman, E. Getmanova, P.J. Reeves, M. Ziliox, H.G. Khorana, M. Sheves, S.O. Smith, J. Biomol. NMR 29 (2004) 11–20.
[175] A.K. Mehta, J. Schaefer, J. Magn. Reson. 163 (2003) 188–191.
[176] C.M. Rienstra, M. Hohwy, L.J. Mueller, C.P. Jaroniec, B. Reif, R.G. Griffin, J. Am. Chem. Soc. 124 (2002) 11908–11922.
[177] M. Baldus, Prog. Nucl. Magn. Reson. Spectrosc. 41 (2002) 1–47.
[178] J. Pauli, M. Baldus, B. van Rossum, H. de Groot, H. Oschkinat, Chembiochem 2 (2001) 272–281.
[179] B.J. van Rossum, F. Castellani, K. Rehbein, J. Pauli, H. Oschkinat, Chembiochem 2 (2001) 906–914.
[180] B.J. van Rossum, F. Castellani, J. Pauli, K. Rehbein, J. Hollander, H.J. de Groot, H. Oschkinat, J. Biomol. NMR 25 (2003) 217–223.
[181] M. Baldus, B.H. Meier, J. Magn. Res. 121 (1996) 65–69.
[182] A. Detken, E.H. Hardy, M. Ernst, M. Kainosho, T. Kawakami, S. Aimoto, B.H. Meier, J. Biomol. NMR 20 (2003) 203–221.
[183] E.H. Hardy, A. Detken, B.H. Meier, J. Magn. Reson. 165 (2003) 208–218.
[184] S.K. Straus, T. Bremi, R.R. Ernst, J. Biomol. NMR 12 (1998) 39–50.
[185] M. Hong, J. Biomol. NMR 5 (1999) 1–14.
[186] A. McDermott, T. Polenova, A. Bockmann, K.W. Zilm, E.K. Paulson, R.W. Martin, G.T. Montelione, E.K. Paulsen, J. Biomol. NMR 16 (2000) 209–219.
[187] A.T. Petkova, M. Baldus, M. Belenky, M. Hong, R.G. Griffin, J. Herzfeld, J. Magn. Reson. 160 (2003) 1–12.
[188] A. Lange, S. Luca, M. Baldus, J. Am. Chem. Soc. 124 (2002) 9704–9705.
[189] B.Q. Sun, C.M. Rienstra, P.R. Costa, J.R. Williamson, R.G. Griffin, J. Am. Chem. Soc. 119 (1997) 8540–8546.
[190] M. Hong, J. Magn. Reson. 136 (1999) 86–91.
[191] B. Reif, B.J. van Rossum, F. Castellani, K. Rehbein, A. Diehl, H. Oschkinat, J. Am. Chem. Soc. 125 (2003) 1488–1489.
[192] Y. Matsuki, H. Akutsu, T. Fujiwara, Magn. Reson. Chem. 42 (2004) 291–300.
[193] R. Verel, M. Ernst, B.H. Meier, J. Magn. Reson. 150 (2001) 81–99.
[194] M. Baldus, A.T. Petkova, J. Herzfeld, R.G. Griffin, Mol. Phys. 95 (2004) 1197–1207.
[195] X.L. Yao, M. Hong, J. Biomol. NMR 20 (2001) 263–274.

[196] V. Chevelkov, B.J. van Rossum, F. Castellani, K. Rehbein, A. Diehl, M. Hohwy, S. Steuernagel, F. Engelke, H. Oschkinat, B. Reif, J. Am. Chem. Soc. 125 (2003) 7788–7789.
[197] D.M. LeMaster, D.M. Kushlan, J. Am. Chem. Soc. 118 (1996) 9255–9264.
[198] A. Lange, K. Seidel, L. Verdier, S. Luca, M. Baldus, J. Am. Chem. Soc. 125 (2003) 12640–12648.
[199] A. Samoson, T. Tuherm, Z. Gan, Solid State Nucl. Magn. Reson. 20 (2001) 130–136.
[200] Y. Ishii, R. Tycko, J. Magn. Res. 142 (2000) 199–204.
[201] I. Schnell, H.W. Spiess, J. Magn. Reson. 151 (2001) 153–227.
[202] A. Bockmann, A. Lange, A. Galinier, S. Luca, N. Giraud, M. Juy, H. Heise, R. Montserret, F. Penin, M. Baldus, J. Biomol. NMR 27 (2003) 323–339.
[203] M. Ernst, A. Detken, A. Bockmann, B.H. Meier, J. Am. Chem. Soc. 125 (2003) 15807–15810.
[204] A.T. Petkova, Y. Ishii, J.J. Balbach, O.N. Antzutkin, R.D. Leapman, F. Delaglio, R. Tycko, Proc. Natl. Acad. Sci. U. S. A. 99 (2002) 16742–16747.
[205] C.P. Jaroniec, C.E. MacPhee, V.S. Bajaj, M.T. McMahon, C.M. Dobson, R.G. Griffin, Proc. Natl. Acad. Sci. U. S. A. 101 (2004) 711–716.
[206] C.P. Jaroniec, J.C. Lansing, B.A. Tounge, M. Belenky, J. Herzfeld, R.G. Griffin, J. Am. Chem. Soc. 123 (2001) 12929–12930.
[207] A.F. Creemers, S. Kiihne, P.H. Bovee-Geurts, W.J. deGrip, J. Lugtenburg, H.J. de Groot, Proc. Natl. Acad. Sci. U. S. A. 99 (2002) 9101–9106.
[208] T.A. Egorova-Zachernyuk, J. Hollander, N. Fraser, P. Gast, A.J. Hoff, H.J.M. de Groot, M. Baldus, J. Biomol. NMR 19 (2001) 243–253.
[209] P.T. Williamson, S. Bains, C. Chung, R. Cooke, A. Watts, FEBS Lett. 518 (2002) 111–115.
[210] S. Luca, J.F. White, A.K. Sohal, D.V. Filippov, J.H. van Boom, R. Grisshammer, M. Baldus, Proc. Natl. Acad. Sci. U. S. A. 100 (2003) 10706–10711.